

An Experimental Study of Cavity Shedding Mechanisms for Unsteady Cloud Cavitation

^{1,2}Qin Wu*; ²Guoyu Wang; ³Mohamed Farhat; ²Biao Huang; ¹Shuliang Cao

¹*Tsinghua University, Beijing, 100084, China;* ²*Beijing Institute of Technology, Beijing, 100081, China;*

³*Ecole Polytechnique Fédérale de Lausanne, 1007 Lausanne, Switzerland*

Abstract

The objective of this work is to shed light on different mechanisms associated to the cloud cavitation instability and corresponding vibration characteristics. Results are presented for a modified NACA66 hydrofoil tested in the EPFL high-speed cavitation tunnel. The high-speed digital camera and the single point Laser Doppler Vibrometer are applied to analyze the unsteady cavitating flow structures and corresponding structural vibration characteristics. For the partial cloud cavitation, it occurs when the maximum cavity length is less than $1.0c$ with Strouhal number of 0.3-0.4. As for the trailing cloud cavitation, the Strouhal number decreases to 0.1-0.15 with the cavity extending to the downstream of the hydrofoil, accompanied with intense vibration and noise. Compared with the cavity shedding dynamics in the partial cloud cavitation, it has a more complex cavitating flow patterns for the trailing cloud cavitation. When the shedding cloud cavity reaches to the rear part of the hydrofoil, it collapses and induces a strong shock wave, which moves backward. As a result, the main cavity shrinks and may even entirely disappears on the suction side. After that, the cavity begins to form and develop again in the next period. Hence, a significant reduction of the shedding frequency and much larger vibration velocities can be observed for the trailing cloud cavitation.

Keywords: cloud cavitation; cavity shedding; flow-induced vibration; experimental study

Introduction

Cavitation generally occurs when the local fluid pressure reduces to the saturated vapor pressure and consequently the gas filled or gas and vapor filled bubbles are formed. For a long time, a large number of experiments [1-4] and numerical simulations [5-7] have been conducted to study the cavitating flow structures and dynamics on hydrofoils. As mentioned in the previous researches, the temporal periodicity may occur as a result of the unsteady break-off and periodical shedding of the large cloud cavities, which will generate significant pressure fluctuations and aggravates the flow-induced vibration of structures, so that it can lead to many problems and become a primary concern for the hydraulic machine and marine engineering [8-10]. Arndt et al. [11-12] investigated the instability of partial cavitation noting the cavity patterns, maximum amplitude in lift and noise characteristics. They found that the vertical extent of the cavitating flow is less at lower angle of attack. Leroux et al. [13-14] observed two distinct cavity self-oscillation dynamics and found that the re-entrant jet was mainly responsible for the cavity breakdown and the strong pressure wave generated by the cloud cavity collapse is responsible for the instabilities. Seo and Lele [15] investigated the partial cavitating flow and cloud cavitating flow with focus on the pressure wave generated by collapse of cloud cavity. The results showed that the pressure pulse generated by the collapse of bubble cloud and the flow-blockage effect caused by a large cloud cavity are responsible for the shifting of cloud cavitation dynamics.

The objective of this work is to analyze different mechanisms associated to the cloud cavitation instability, in particular, to further explore the stable partial cloud cavitating and the unstable trailing cloud cavitating flow regimes. In this paper, the experimental setup and the measuring techniques are first presented. Then the typical vibration characteristics along with corresponding cavitation patterns are given. Finally, the conclusions are summarized in the last section.

Experimental setup and methods

The experimental studies are conducted in the high-speed cavitation tunnel in EPFL [16], as shown in Fig. 1. The test section is 0.7m (length) \times 0.07m (width) \times 0.19m (height), with the free stream turbulence intensity around 2%. As sketched in Fig. 2, the test hydrofoil is a modified-NACA66 made of stainless steel, which has a uniform cross-section of shape with chord length $c=0.1\text{m}$, the span $b=0.15\text{m}$ and a maximum thickness-to-chord ratio of 12%. The flow

conditions are set based on the Reynolds number $Re=U_\infty c/\nu=1.0\times 10^6$, where U_∞ is the free stream velocity, ν is the dynamic viscosity of the liquid, and the cavitation number $\sigma=(p_\infty-p_v)/(0.5\rho U_\infty^2)$, where p_∞ is the pressure in the test section, p_v is the saturated vapor pressure at ambient temperature, ρ is the liquid density.

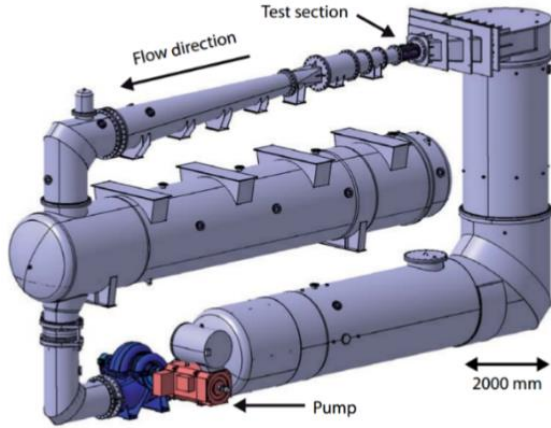


Figure 1 Cavitation tunnel

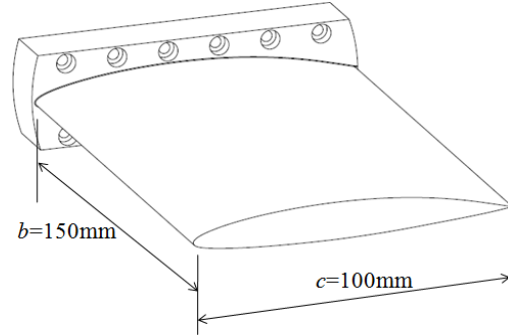


Figure 2 NACA66 hydrofoil

The cavitation patterns are visualized by a Photron Fastcam SA1.1 digital camera from the front (704×400 pixels) and top (576×480 pixels) of the section at a sampling rate of 20000 frames per second. The flow-induced vibration is measured with a laser Doppler vibrometer, Polytec PDV100. The sample frequency of 5kHz is adopted in the present work and the smallest possible measurement range is used to optimize the signal-to-noise ratio. The measurement point is focused on the pressure side of the hydrofoil at the position of $x/c = 0.75$ and $z/b = 0.6$, where the vibration signal is strong enough without interfere of the cavity formed on the suction side and wake region of the hydrofoil. The data acquisition system is controlled by a NI-Labview programming and a sampling frequency of 5kHz is adopted in this work. For frequency spectral analysis, Fast Fourier Transform is applied to 30 equal segments of the time signals with 50% overlap between the adjacent segments, followed by averaging of the spectrum, so the time and frequency resolutions are 0.0002s and 0.5Hz respectively.

Results and discussions

As to the regime of the cloud cavitation, the unsteady breakdown and shedding of the cavity occurs violently, which may lead to strong dynamic instabilities. The visualization of two typical cavitation development, trailing cloud cavitation ($\alpha=6^\circ$, $\sigma=1.2$, $\sigma/2(\alpha-\alpha_0)=4.58$) and partial cloud cavitation ($\alpha=8^\circ$, $\sigma=1.5$, $\sigma/2(\alpha-\alpha_0)=4.52$), is shown in Figs. 3 and 4. Figure 5 shows the evolution of the cavity lengths in two consecutive cycles, which are extracted from the recorded images. The cavity growth rate is changing through the whole cavitation developing process. The periodical formation and shedding of large-scale cloud cavity can be captured in both cases, but compared to the cavity patterns for the partial cloud cavitation, the cavity shedding process for the trailing cloud cavitation is more complex and characterized by a lower frequency.

For the trailing cloud cavitation, at first, the partial sheet cavity forms and develops on the suction side of the hydrofoil, along with formation of the re-entrant jet at the rear end of the cavity, as shown in Figs. 3(a)-(b), which causes the oscillating of the cavity length in the range of $0.2c$, as shown in Fig. 5(a). When the cavity develops to $0.9c-1.0c$, the trailing end of the cavity becomes unstable and the latter part of the cavity from $0.5c$ to $0.9c$ rolls into cloud cavity cluster due to the interaction between the re-entrant jet and the cavity interface, cutting the cavity length into $0.5c$, as shown in Figs. 3(c)-(d) and Fig. 5(a). With the shedding of the cloud cavity cluster, the residual attached cavity continue growing with a larger cavity growth rate, as shown in Figs. 3(d)-(e) and Fig. 5(a), because the cavity is lifted away from the near surface by the re-entrant jet and the frictional resistance reduces. As the shedding cloud cavity moves downstream of the hydrofoil, it collapses due to the pressure gradient between the flow field and the inner part of the cavity, as shown in Fig. 3(e). Almost at the same time, the residual cavity stops to grow and on the contrary, it shrinks dramatically and even disappears entirely on the suction side, as shown in Figs. 3(f)-(h), corresponding to the sudden decrease of cavity length seen in Fig. 5(a).

As for the partial cloud cavitation, the partial sheet cavity develops from the leading edge of the foil to the position of $x/c=0.8$, as shown in Figs. 4(a)-(f) and Fig. 5(b). During the cavity developing process, the re-entrant jet forms at the rear end of the cavity and moves from both side of the trailing edge of the cavity towards the center of the leading edge of the cavity. The collision of these two bundles of upward flow cuts off the downstream part of cavity and induces the shedding of the cloud cavity, generating a wedge-shape hole at the rear part of the remaining sheet cavity, as shown in Fig. 4(g).

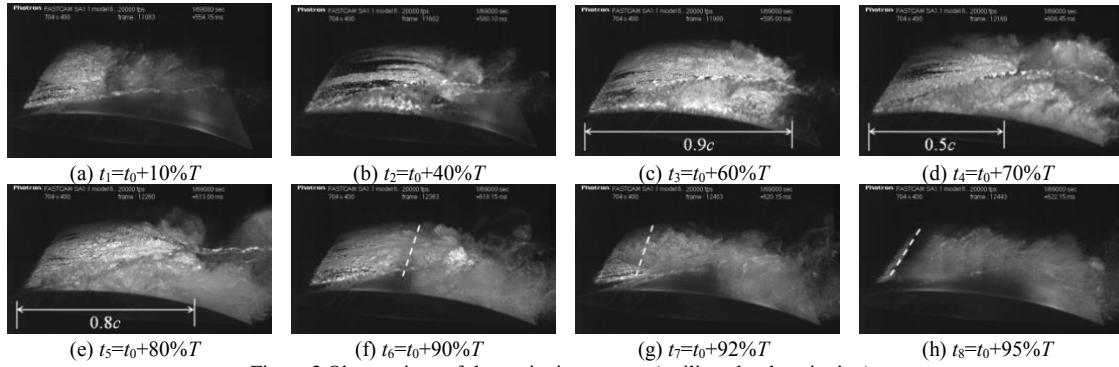


Figure 3 Observations of the cavitation pattern (trailing cloud cavitation)

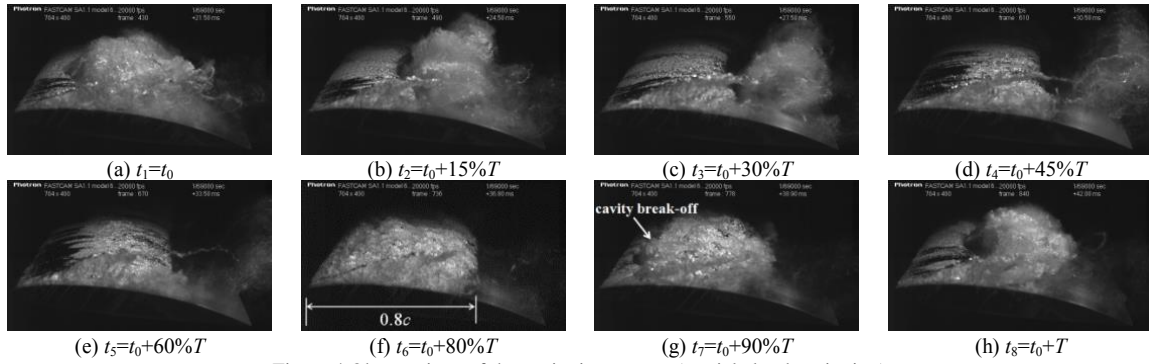


Figure 4 Observations of the cavitation pattern (partial cloud cavitation)

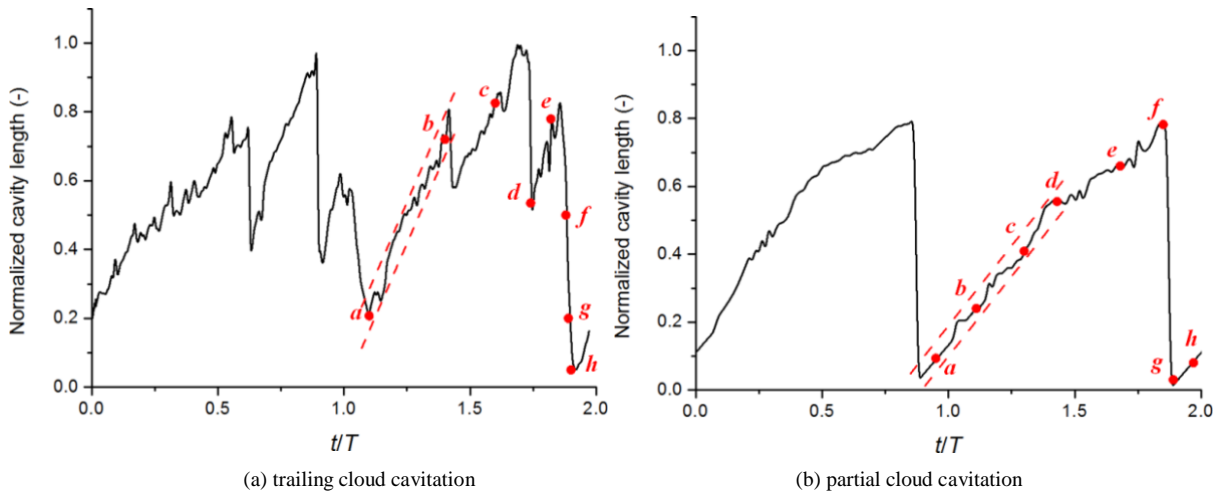


Figure 5 Evolution of the cavity lengths

Figure 6 shows the time evolution of the vibration velocity for the cases with trailing cloud cavitation and partial cloud cavitation. Hilbert transform is applied to determine the envelop of the vibration signals. The vibration signals for both cases exhibit marked periodic variation, but the vibration amplitude for the trailing cloud cavitation is much larger. Also noted in Fig. 6, for the trailing cloud cavitation, each period of oscillation consists of distinct two parts, small

amplitude fluctuations accompanied with the increase of the envelop of the vibration signals and large amplitude fluctuations together with the decrease of the vibration signals envelop curve. While for the partial cloud cavitation, the vibration velocity goes up and down periodically with small amplitude fluctuations. Based on the Hilbert transform, the spectra for these two cavitating flow regimes is shown in Fig. 7. The dominant frequencies for the trailing cloud cavitation and partial cloud cavitation are 14Hz and 44Hz respectively.

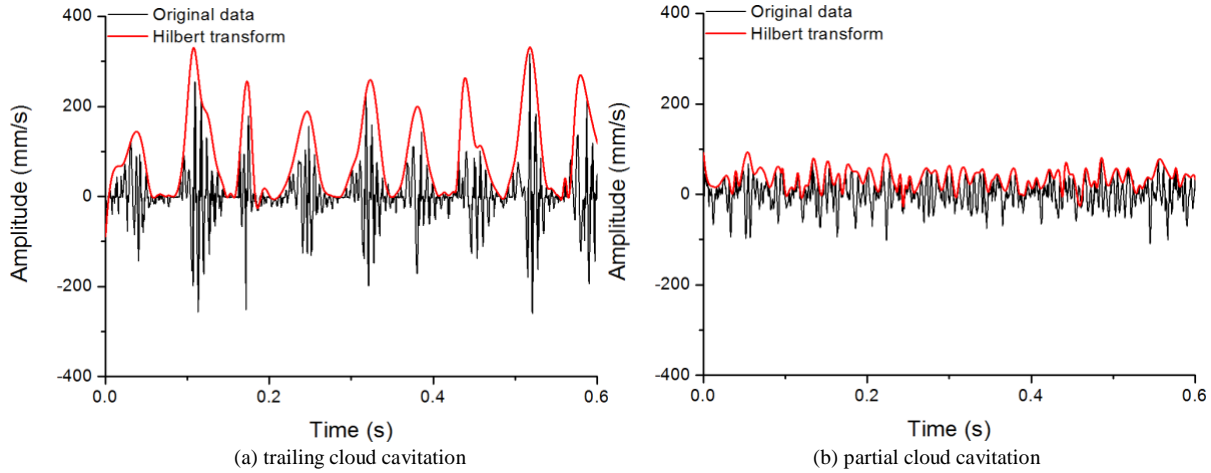


Figure 6 Time evolution of the vibration velocities

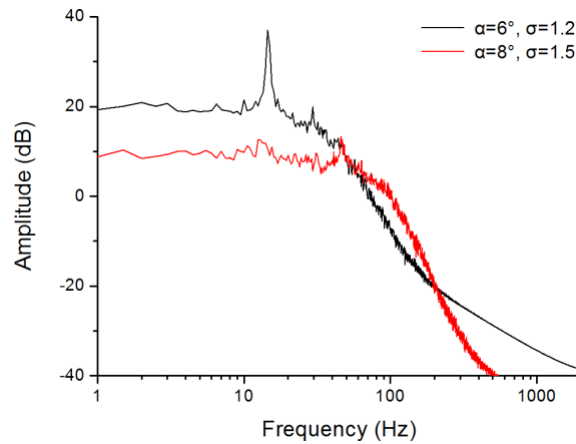


Figure 7 Spectrum analysis of the vibration velocities

Comparing the shedding process occurred in both cases, it can be seen that there are two competing mechanism acting on the cavity shedding. One is the re-entrant jet due to the pressure gradient at the rear end of the cavity, as seen in Fig. 3(b) and Fig. 4(d). The other is the shock wave induced by the collapse of the cloud cavity, as seen in Figs. 3(f)-(h) and Figs. 4(d)-(e). When the maximum cavity length is larger than $1.0c$, the collapse of the cavity occurs in the downstream of the hydrofoil and the pressure difference between the suction side and pressure side of the hydrofoil aggravates the pressure gradient between the inner and outer region of the cavity, so that the shock wave induced by the collapse dominates the evolution of the cavity structures, which is corresponding to the larger amplitude fluctuation of the vibration velocities shown in Fig. 5.

Conclusion

In this paper, experiments on a modified NACA66 hydrofoil in cloud cavitating flow have been conducted based on high speed photography and laser vibrometry. Two typical cavity patterns and the corresponding vibration characteristics are analyzed.

For the partial cloud cavitation, with the maximum cavity length less than 1.0 and the Strouhal number of 0.3-0.4, the partial sheet cavity forms and develops on the suction side of the hydrofoil with the formation of the re-entrant jet at the rear end of the cavity, as the re-entrant jet flowing toward the leading edge of the hydrofoil, the cavity is lifted away from the near surface and a large-scale cloud cavity breaks up with the main cavity and sheds downstream, accompanied with the growth of the residual cavity on the suction side of the hydrofoil.

For the trailing cloud cavitation, the cavity extends to the downstream of the hydrofoil and the Strouhal number decreases to 0.1-0.15 accompanied with intense vibration and noise. A more complex cavitating flow pattern is observed. When the shedding cloud cavity reaches to the rear part of the hydrofoil, it collapses and induces a strong shock wave. As a result, the main cavity shrinks and may even entirely disappears on the suction side. Compared with the partial cloud cavity shedding dynamics ($St=0.3-0.4$), a significant reduction of the shedding frequency can be observed, which results to a much lower Strouhal number ($St=0.1-0.12$), and larger vibration velocities were obtained.

Acknowledgments

The authors gratefully acknowledge the support by the National Postdoctoral Program for Innovative Talents (Grant No: BX201700126), the China Postdoctoral Science Foundation (Grant No: 2017M620043), the National Natural Science Foundation of China (Grant No: 51679005) and the National Natural Science Foundation of Beijing (Grant No: 3172029).

References

- [1] Wang, G. Y., Senocak, I., Shyy, W., Ikohagi, T., Cao, S. L. (2001) *Dynamics of attached turbulent cavitating flows*. Progress in Aerospace Sciences. 37.
- [2] Foeth, E. J., Van Doorne, C. W. H., Van Terwisga, T., Wieneke, B. (2006) *Time resolved PIV and flow visualization of 3D sheet cavitation*. Experiments in Fluids. 40.
- [3] Ausoni, P., Farhat, M., Escaler, X., Egusquiza, E., Avellan, F. (2007) *Cavitation Influence on von Kármán Vortex Shedding and Induced Hydrofoil Vibrations*. Journal of Fluids Engineering. 129.
- [4] Wu, Q., Wang, Y., Wang, G. (2017) *Experimental investigation of cavitating flow-induced vibration of hydrofoils*. Ocean Engineering. 144(1).
- [5] Coutier-Delgosha, O., Reboud, J. L., Dellanoy, Y. (2003) *Numerical simulation of the unsteady behaviour of cavitating flows*. International Journal of Numerical Methods in Fluids. 42.
- [6] Huang, B., Zhao, Y., Wang, G. Y. (2014) *Large eddy simulation of turbulent vortex-cavitation interactions in transient sheet/cloud cavitating flows*. Computers & Fluids. 92.
- [7] Kubota, A., Kato, H., Yamaguchi, H. (1992) *A new modelling of cavitating flows: a numerical study of unsteady cavitation on a hydrofoil section*. Journal of Fluid Mechanics. 240
- [8] Arndt, R. E. A. (1981) *Cavitation in fluid machinery and hydraulic structures*. Annual Review of Fluid Mechanics. 3.
- [9] Luo, X., Ji, B., Tsujimoto, Y. (2016) *A review of cavitation in hydraulic machinery*. Journal of Hydrodynamics. 28.
- [10] Wu, Q., Wang, G., Huang, B., Gao, Y. (2015) *Experimental and numerical investigation of hydroelastic response of a flexible hydrofoil in cavitating flow*. International Journal of Multiphase Flow. 74.
- [11] Arndt, R. E. A. (2012) *Some remarks on hydrofoil cavitation*. Journal of Hydrodynamics. 24(3).
- [12] Arndt, R. E. A., Song, C. C. S., Kjeldsen, M., Keller, A. (2000) *Instability of partial cavitation: A numerical/experimental approach*. Proceedings of 23rd Symposium for Naval Hydrodynamics.
- [13] Leroux, J. B., Coutier-Delgosha, O., Astolfi, J. A. (2005) *A joint experimental and numerical study of mechanisms associated to instability of partial cavitation on two-dimensional hydrofoil*. Physics of Fluids. 17.
- [14] Leroux, J. B., Astolfi, J. A., Billard, J. Y. (2004) *An experimental study of unsteady partial cavitation*. Journal of Fluids Engineering. 126.
- [15] Seo, J. H., Lele, S. K. (2009) *Numerical investigation of cloud cavitation and cavitation noise on a hydrofoil section*. Proceedings of 7th Symposium of Cavitation. CAV2009-0062.
- [16] Avellan, F., Henry, P., Rhyming, L. (1987) *A new high speed cavitation tunnel for cavitation studies in hydraulic machinery* ASME Fluids Engineering Division FED. 57.